Kaneko *et al. Earth, Planets and Space* (2016) 68:72
DOI 10.1186/s40623-016-0452-y

Earth, Planets and Space

FULL PAPER

Open Access

2014 Mount Ontake eruption: characteristics of the phreatic eruption as inferred from aerial observations

Takayuki Kaneko*, Fukashi Maeno and Setsuya Nakada

Abstract

The sudden eruption of Mount Ontake on September 27, 2014, led to a tragedy that caused more than 60 fatalities including missing persons. In order to mitigate the potential risks posed by similar volcano-related disasters, it is vital to have a clear understanding of the activity status and progression of eruptions. Because the erupted material was largely disturbed while access was strictly prohibited for a month, we analyzed the aerial photographs taken on September 28. The results showed that there were three large vents in the bottom of the Jigokudani valley on September 28. The vent in the center was considered to have been the main vent involved in the eruption, and the vents on either side were considered to have been formed by non-explosive processes. The pyroclastic flows extended approximately 2.5 km along the valley at an average speed of 32 km/h. The absence of burned or fallen trees in this area indicated that the temperatures and destructive forces associated with the pyroclastic flow were both low. The distribution of ballistics was categorized into four zones based on the number of impact craters per unit area, and the furthest impact crater was located 950 m from the vents. Based on ballistic models, the maximum initial velocity of the ejecta was estimated to be 111 m/s. Just after the beginning of the eruption, very few ballistic ejecta had arrived at the summit, even though the eruption plume had risen above the summit, which suggested that a large amount of ballistic ejecta was expelled from the volcano several tens-of-seconds after the beginning of the eruption. This initial period was characterized by the escape of a vapor phase from the vents, which then caused the explosive eruption phase that generated large amounts of ballistic ejecta via sudden decompression of a hydrothermal reservoir.

Keywords: Volcano, Aerial observation, Ballistics, Impact crater, Ontake, Phreatic eruption

Background

Mount Ontake in central Japan erupted on September 27, 2014 (Fig. 1). The sudden eruption led to a tragedy in which more than 60 hikers on the mountain were killed or went missing. Since the eruption was small and terminated within a short period, details of the mechanisms responsible for hazardous eruptions such as this remain unknown. However, in order to mitigate such volcano-related disasters, we need a thorough understanding of the activity status and stages of progression of volcanic activity.

Mount Ontake erupted for the first time in recorded history in 1979 (Kobayashi 1980), and since then, small phreatic eruptions occurred in 1991 and 2007 (Oikawa 2008; Oikawa et al. 2014). On September 10 and 11, 2014, the frequency of tremors under the volcano increased before subsiding again on September 12 (Japan Metrological Agency (JMA) 2014). Then, at 11:52 on September 27, the volcano erupted suddenly from a vent in the Jigokudani valley on the southern side of the summit (JMA 2014). The volcanic tremors that began 11 min before the eruption were followed by rapid inflation of the edifice 4 min later (JMA 2014). The eruption plume, which resembled cumulonimbus clouds, finally reached a height of approximately 11 km above sea level (ASL; Sato et al. 2015), and pyroclastic flows flowed down the slopes. The ballistic ejecta that were generated were considered

*Correspondence: kaneko@eri.u-tokyo.ac.jp
Earthquake Research Institute, The University of Tokyo, 1-1-1 Yayoi, Bunkyoku, Tokyo 113-0032, Japan

to be the main cause of the many casualties, according to comments from the local hospital (Nagano Prefectural Kiso Hospital). Metrological radar observations indicated that the explosive phase ceased around 12:40 (Sato et al. 2015). As with previous eruptions, the 2014 eruption was considered to be a phreatic eruption, as no fresh magma was contained (Oikawa et al. 2015).

This paper attempted to interpret the status and progression of the volcanic activity associated with the 2014 Mount Ontake eruption through aerial observations and to analyze the eruptive processes and mechanisms associated with the phreatic eruption that resulted in the disaster on Mount Ontake.

Methods

In this study, analyses of the eruption processes based on erupted materials were complicated by the extensive disturbance and disruption of the original structure of the deposits that were due to the extensive rescue operations and rainfall following the eruption. Specifically, rescue efforts involved extensive excavation of the deposits near the summit, and the rains disrupted large amounts of tephra and ejected materials during the one-month period when access to the site by volcanologists was strictly prohibited. We therefore focused our analysis on aerial photographs taken immediately after the eruption, as these preserved the original situation and structure of the erupted materials and topography, both of which are important for elucidating eruption processes. On September 28, the day following the eruption, between 13:54 and 15:15, one of us (TK) surveyed the volcano from a media helicopter (Chunichi/Tokyo Shimbun Newspaper Co.) and took more than 350 images of the areas affected by the eruption with a digital camera (SONY DSC-RX100M2). In addition to these photographs, we also used many images and videos of the eruption that were captured by hikers and members of the mass media. Together with the eyewitness testimonies, the image information was useful for inferring and refining the temporal relationships among the events associated with the eruption.

Results: characteristics of vents and depositional areas inferred from aerial observations

Distribution and characteristics of the eruption vents

The eruption vents produced by the 2014 eruption were located on the southwestern side of the summit and oriented along a west-northwest to east-southeast axis (Figs. 1b, 2a). The three vent areas included the W1 vent and fissures on the western slope of the Ichinoike cone, the J1–J7 vents in the Jigokudani valley, and the E1 vent west of Ohtakisancho peak. Although the location and general orientation of the vents were similar to those for the 1979 eruption, they had shifted 200–300 m to the south-southwest and had extended by about 300 m to the west-northwest.

Three large, adjacent vents (J3–J5) that appeared to be connected were located on the floor of the Jigokudani

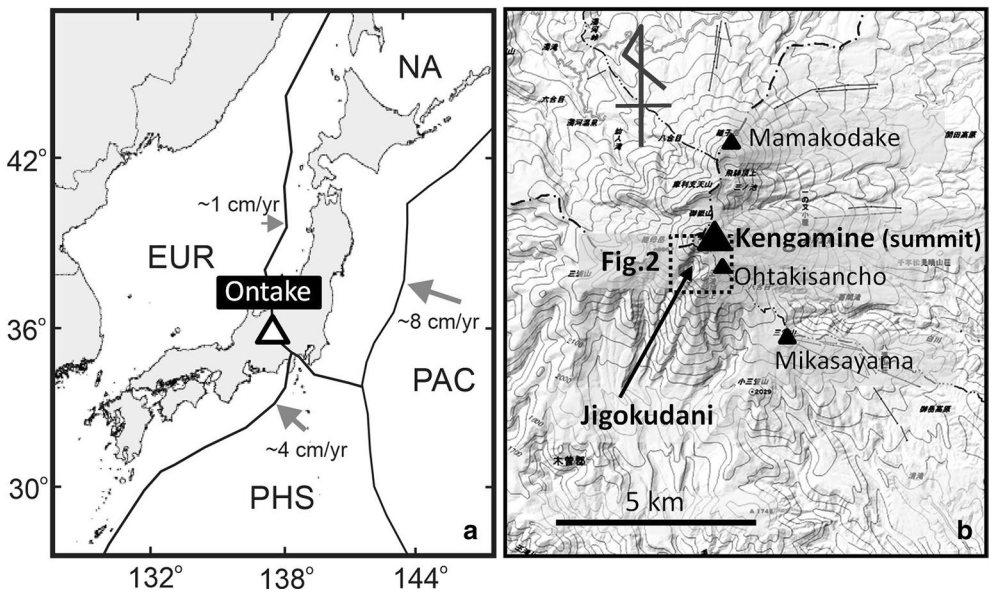

Fig. 1 **a** Location of Mount Ontake. *PAC* Pacific plate, *PHS* Philippine Sea plate, *NA* North America plate, *EUR* Eurasian plate. **b** Topography of Mount Ontake. Kengamine is the summit of Mount Ontake (3067 m ASL). The topographic base map was produced using a GSI map issued by the Geospatial Information Authority of Japan

valley. On September 28, three smaller vents (J1–J2 and J6) were observed on the valley wall (Figs. 2a, 3e; the J7 vent was inactive on the 28th). The large vents were associated with piles of pyroclastic materials and formed a pyroclastic cone on the southern slope of the valley. In the photograph taken at 14:13 on September 27 (Figs. 2b, 3a), the J4 vent appeared as it was on September 28 (Figs. 2a, 3e); however, the J3 vent appeared somewhat smaller in size, and the J5 vent could not be identified. In the photograph taken at 15:11 (Fig. 3b), the J3 vent was larger in size, reaching its final shape in the photographs taken at 16:02 (Fig. 3c), and parts of the J5 vent could be recognized near the eastern side of the valley wall (Fig. 3c). Thus, these two vents are considered to have formed between 14:13 and 16:02 on September 27. Because no explosive eruption occurred during that time, they are considered to have been generated by non-explosive processes such as the collapse of a part of the vent area into the conduit. Thus, it is likely that the J4 vent was the main vent involved in the eruption on September 27. In the photograph taken at 16:44 (Figs. 2c, 3d), a mudflow was observed on the slope of the pyroclastic cone. The mudflow appeared to have effused between 16:02 and 16:44. In the image taken on September 28, the interior of the J4 vent appeared dark, suggesting that it was filled with mud or water. In addition, a rill-like structure formed on the slope of the pyroclastic cone (Fig. 3e, f), probably due to erosion caused by repeated mudflows from the vent. Small-scale mudflows were also observed, which probably effused from other very small vents and fractures (Fig. 3a, b).

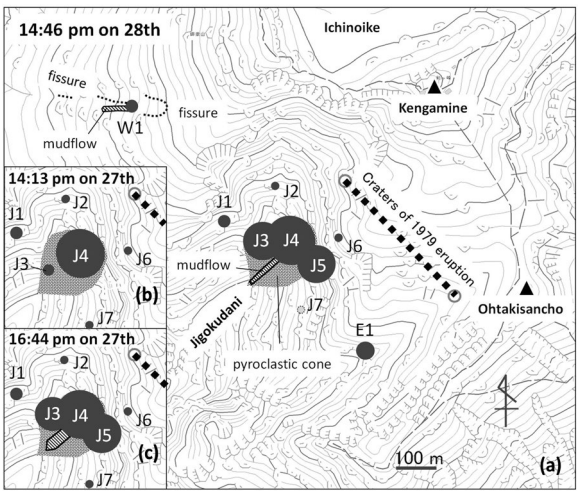

Fig. 2 **a** Distribution of the eruption vents on September 28, 2014. **b** Eruption vents in the Jigokudani valley at 14:13 on September 27 and **c** at 16:44 on September 27. The topographic base map was produced using a GSI map issued by the Geospatial Information Authority of Japan

On the western slope of the Ichinoike cone, the fissures generated were arranged along an east–west trending axis, with the W1 vent in the center (Fig. 2a). Although the W1 vent was not surrounded by a pile of pyroclastic materials, it ejected a fine brownish ash layer that covered the surrounding areas, particularly to the north. In addition, a mudflow was observed to have effused from the vent (Fig. 4). All of the fissures emitted fumarolic gas. The E1 vent located 400 m west of Ohtakisancho peak (Fig. 2a) may have ejected ballistic materials over the surrounding areas, but pyroclastic materials did not appear to have collected around it.

Distribution and characteristics of the pyroclastic flows

Pyroclastic flow-like units occurred during this eruption. Although no examples of pyroclastic flow typical of magmatic eruptions were observed, flows comprising a mixture of ash and gas moved down the slope by gravity (Yamamoto 2014). We referred to these as "pyroclastic flows."

Based on images captured by hikers (e.g., Asahi 2014), when the initial eruption plume reached an altitude of several hundred meters above the summit, the plume began to expand laterally before flowing down the volcano slopes as pyroclastic flow in almost all directions. Because the temperature of the plume was relatively low, the entire plume may not have been able to rise very high above the volcano. Based on the time at which the dense ashy plume that covered the cottage at the summit had disappeared (Kaito 2014), pyroclastic flows are considered to have been generated intermittently until around 12:20 on September 27. Video footage taken by a hiker who was caught in moving pyroclastic flow (https://www.youtube.com/watch?v=GGTp0bNb608) revealed that the flow consisted of aggregated ash particles blowing laterally as in a snow storm. The majority of the pyroclastic flow deposits were distributed within approximately 1 km of the vents, except in the area southwest of the vent (Fig. 5a).

The pyroclastic flow moved away from the vent in a southwesterly direction along the Jigokudani valley for approximately 2.5 km, as this area was lower than the surrounding areas (Fig. 5a, b). Areas affected by the pyroclastic flow appeared whitish because of the presence of ash on vegetation (Fig. 5d). The absence of burned or fallen trees implied that the temperatures and forces associated with the pyroclastic flow events were both low.

Camera footage recorded by the Ministry of Land, Infrastructure, Transport and Tourism, taken from near Takigoshi village on the southern foot of the volcano (http://www.cbr.mlit.go.jp/tajimi/sabo/ontake/, https://www.youtube.com/watch?v=jt36uloZ3oI), revealed that the pyroclastic flow reached a distance of 2.5 km

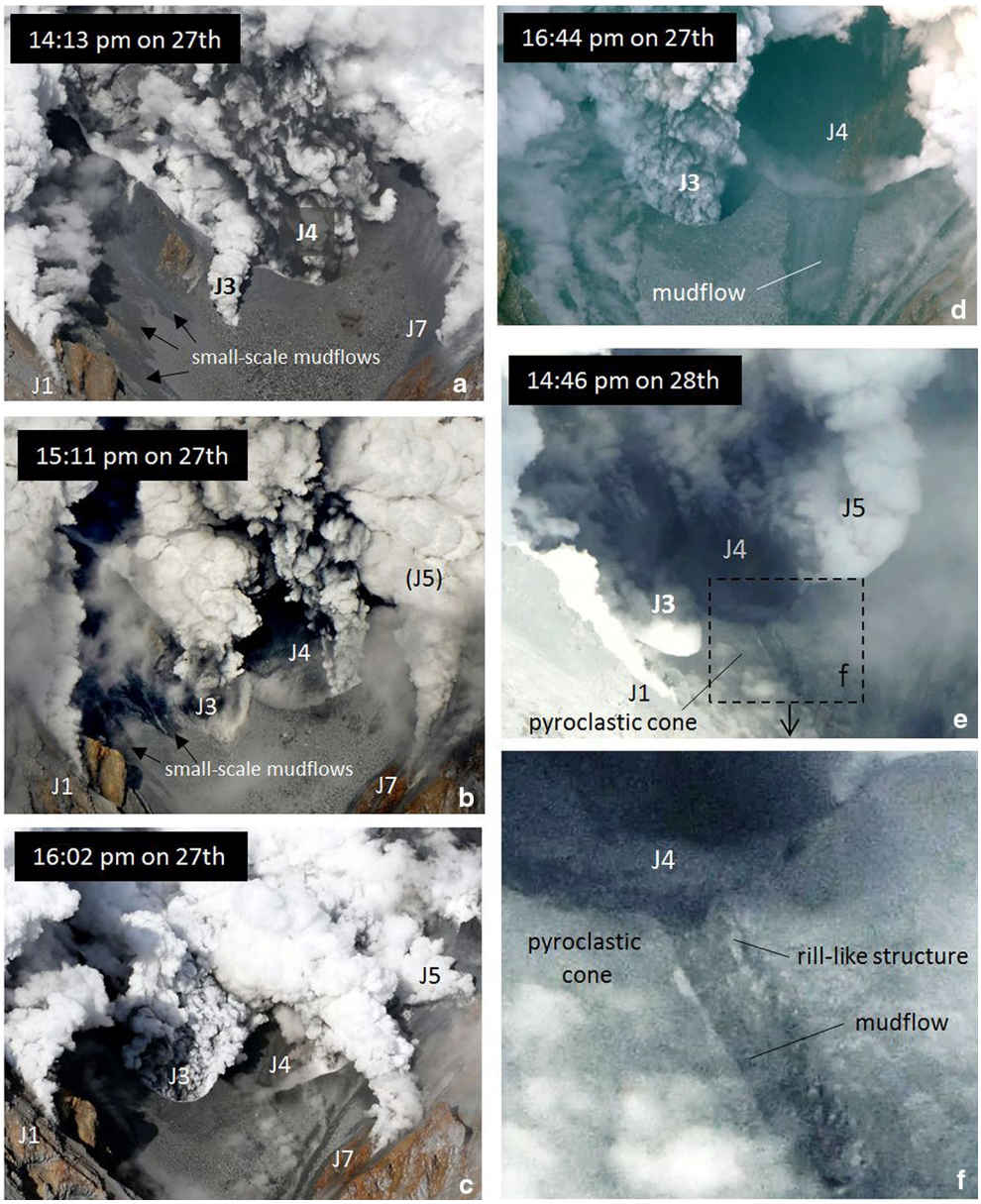

Fig. 3 Photographs of the eruption vents in the Jigokudani valley at **a** 14:13 on September 27 (Asahi Shimbun), **b** 15:11 on September 27 (The Mainichi), **c** 16:02 on September 27 (Asahi Shimbun), **d** 16:44 on September 27 (Asahi Shimbun), and **e** 14:46 on September 28 (J2 and J6 are not visible in this photograph). **f** Close-up of a rill-like structure that originated from the J4 vent

away from the vent at 11:57 about 5 min after the beginning of the eruption. The front of the pyroclastic flow passed through the point of an altitude of 2500 m of the Jigokudani valley around 11:53; thus, it traveled 2.1 km in 4 min. This means that the pyroclastic flow in this area moved at an average speed of 32 km/h (8.8 m/s), which is considered slow for pyroclastic flow (see Cas and Wright 1987). Indeed, the pyroclastic flows observed in this study could be considered a kind of pyroclastic surge that is characterized by low speed and low temperature. Similar pyroclastic flows were also observed in the phreatic eruption of Miyakejima on August 29, 2000 (Nakada et al. 2005), indicating that this kind of pyroclastic flow might be typical of low-temperature, phreatic eruptions with no magmatic material in the ejecta.

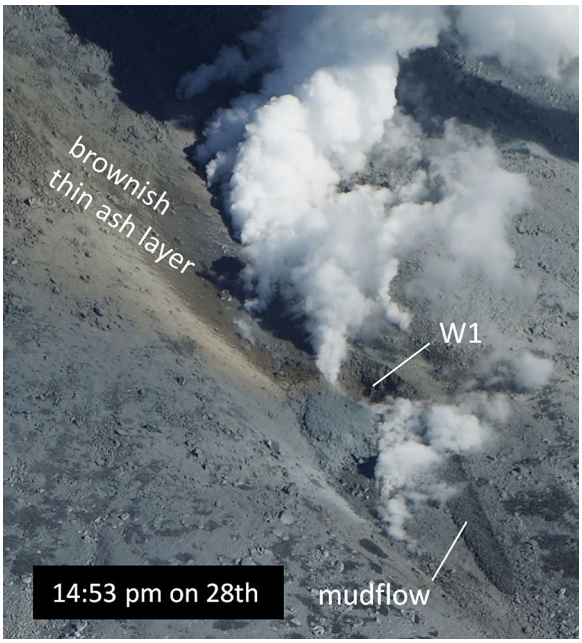

Fig. 4 Photographs of the eruption vents and fissures on the western slope of the Ichinoike cone, taken at 14:53 on September 28

Distribution and characteristics of the air-fall deposits

The height of the eruption plume increased over time and, based on metrological radar observations, was inferred to have reached an altitude of approximately 11 km around 12:10 (Sato et al. 2015). Although the plume, precipitating ash over an extensive area, tilted toward the northeast at low altitudes, it moved east-northeast at high altitudes. A mixture of air-fall and pyroclastic flow deposits appears to have settled in the vicinity of the summit.

The depositional axis of the air-fall ash, indicated by a whitish color on the ground, extended to the east-northeast (Fig. 5a, c). The arrow labeled "e" in Fig. 5c indicates air-fall ash deposits comprising fine ash particles aggregated with accretionary lapilli (Fig. 5e); the thickness of this layer was 2–3 mm, and the size of the particles was 1–2 mm.

At the summit of Ichinoike, which was covered by a thick layer of ashy deposits, sun cracks developed on the surface (Fig. 5f), and water collected in the bottom of the impact craters on the day after eruption, even in those on part of the inner wall of the Ichinoike cone (Fig. 5g). These findings reveal that the ash (air-fall/pyroclastic flow) was enriched with water components, corroborating the observation of accretionary lapilli. According to a hiker at the summit, although the ash was initially dry, it became wetter, taking on the form of "mud rain" in the final stages (Kaito 2014). In video footage taken immediately after the eruption (https://www.youtube.com/watch?v=ODiqlpUwcVM), the top 1–2 cm of the few tens-of-centimeters of ash that was deposited near the summit appeared wet and semisolid, looking dark in color. This water is considered to have been derived from the precipitation of water vapor contained in the eruption plume.

Distribution of ballistic ejecta

The phreatic eruption of Mount Ontake generated large amounts of ballistic ejecta. According to a hiker who sought shelter in the cottage at the summit, the generation of ejecta continued intermittently for about 1 h (Kato 2014). This report is concordant with the morphological variation observed in the impact craters produced by the ballistic ejecta, which included craters with both well-defined and indistinct outlines (Fig. 5f).

Instead of actual ballistic ejecta, which are difficult to identify directly, the distribution of ballistic ejecta was inferred based on the distribution of impact craters in the photographs taken on September 28 (Figs. 6, 7). Impact craters were identified based on the outline and concave topography suggested by the effect of shading in the photographs. In each photograph, the scale of the scene was estimated by matching characteristic topographic features including large rocks to the locations on topographic map using Google Maps/Google Earth and GSI Maps (Geospatial Information Authority of Japan—http://maps.gsi.go.jp). Based on the estimated scales, 5×5 m areas were selected on each photograph to count the number of impact craters (Fig. 7). The size of impact craters and ballistics was also estimated based on the scale obtained here and characteristic objects in the same scene, such as statues, monuments, stone stairs, or rescue workers.

The diameters of impact craters ranged between several tens-of-centimeters to 1 m, while those of ballistic ejecta ranged from 10 cm to several tens-of-centimeters (maximum c. 1 m). The distribution density was classified into four zones, based on the number of craters per unit area (5×5 m); these zones were called Zones A, B, C, and D, with Zone A having the highest density of impact craters and Zone D having no impact craters. Because the distribution density of craters decreased with increasing distance from the vents, the distribution density was very high between Kengamine and Ichinoike (Fig. 7, Zone A ①–③). The furthest impact crater was located at Ninoike pond, 950 m from the vents in the Jigokudani valley (Fig. 7, Zone C ⑨). We were unable to survey the distribution of impact craters in the area to the south of the vents because they were obscured by the volcanic plume at the time the observations were made,

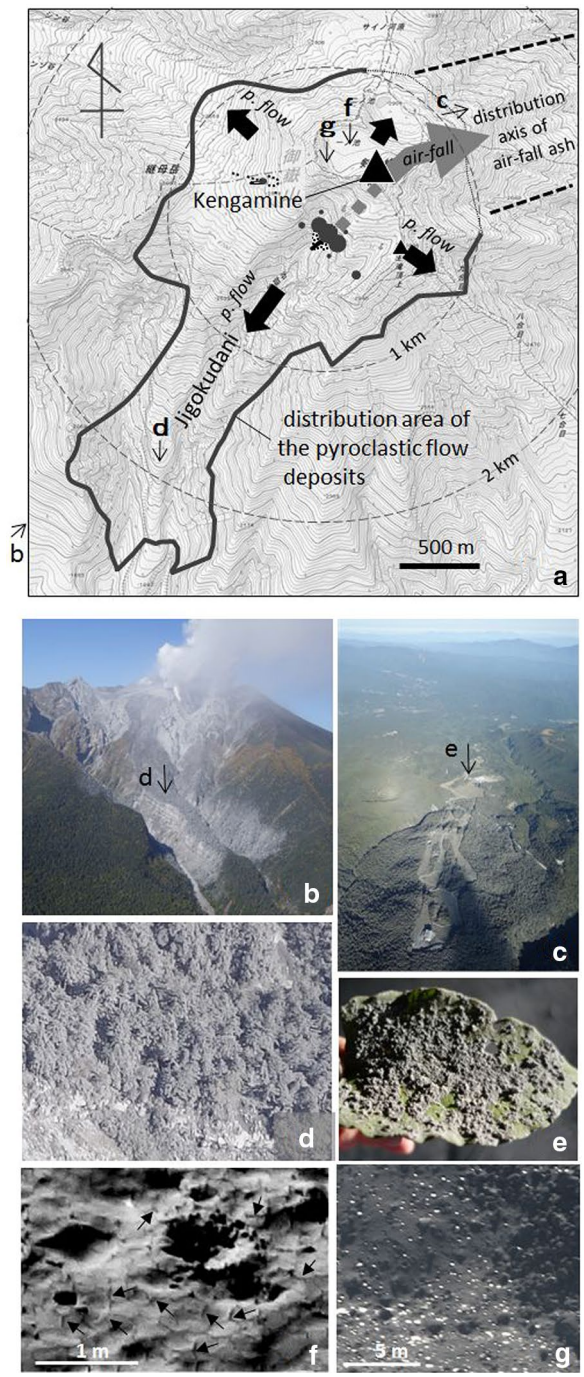

Fig. 5 **a** Distribution of pyroclastic flow deposits and air-fall ash. **b**, **c**, **d**, **f**, **g** with *small arrows* show the direction or location where **b**, **c**, **d**, **f**, **g** were taken, respectively. **b** The Jigokudani valley viewed from the southwest on September 28. **c** Distribution axis of air-fall ash extending to the north-northeast, viewed from above the Ninoike cone on September 28. **d** Close-up of the depositional area of the pyroclastic flow on September 28. **e** Air-fall ash deposited on a leaf, taken on the evening of September 27 (120 m east-northeast of Shikano-yu ropeway station). **f** Impact craters and sun cracks (representative cracks are suggested by *arrows*) that developed on the ash deposits in Ichinoike on September 28. **g** Impact craters on the inner wall of the Ichinoike cone, most of which contained water at the bottom and appear to be glistening white because of reflected sunlight. The topographic base map was produced using a GSI map issued by the Geospatial Information Authority of Japan

and the deposition of ash layer was too thin to leave clear crater structures by impact.

The distribution of craters was not isotropic but slightly extended in a north-northeasterly direction (dotted line in Fig. 6). Because the Jigokudani valley extends along a north-northeast to south-southwest axis, and because the vents are located on the valley floor, it is possible that the valley walls acted as barriers to ejecta, preventing ballistics from being ejected far beyond the valley walls along both sides of the valley.

Discussion: occurrence of ballistic ejecta and mechanism of phreatic eruption

Estimation of the initial velocity of ballistic ejecta

Initial velocity estimates for ballistic ejecta were made based on their distribution. The furthest impact crater was located 950 m from the J4 vent in the Jigokudani valley; however, it was reported that ballistic ejecta reached the Ninoike-Honkan cottage approximately 1000 m north-northeast of the vents. Assuming an ejection angle of 45° and a horizontal travel distance of 1000 m, the initial velocity was estimated to be 99 m/s based on a simple ballistic trajectory calculation without air resistance and vertical dip. Assuming that the ejection angles were random, this estimate is considered to reflect the maximum initial ejecta velocity. More precisely, because the J4 vent was located at an altitude of 2750 m and the point of impact—the Ninoike-Honkan cottage—was at 2900 m, the maximum initial velocity was estimated to be 111 m/s with an ejection angle of 49° (Fig. 8a) using the ballistic calculator software "Eject!" (Mastin 2008). In this calculation, the following conditions were used: block shape, sphere; density, 2500 kg/m^3; diameter, 0.2 m; speed of tailwind, 0 m/s; extent of zone of reduced drag, 0 m; temperature at sea level, 25 °C; and thermal lapse rate, 6.5 °C/km. The value for the diameter was adopted in reference to the size of the ballistic that hit the Ninoike-Honkan cottage (17 cm, Cabinet Office 2015). Here, even if we assumed the diameter to be 1 m, the estimated initial velocity would be 108 m/s. Compared to some magmatic eruptions, the maximum initial velocity and the maximum distance estimates associated with this eruption are relatively small. For example, ballistic ejecta generated by the 2011 Shinmoedake eruption traveled 3.4 km and had initial velocities of 240–290 m/s (Maeno et al. 2013).

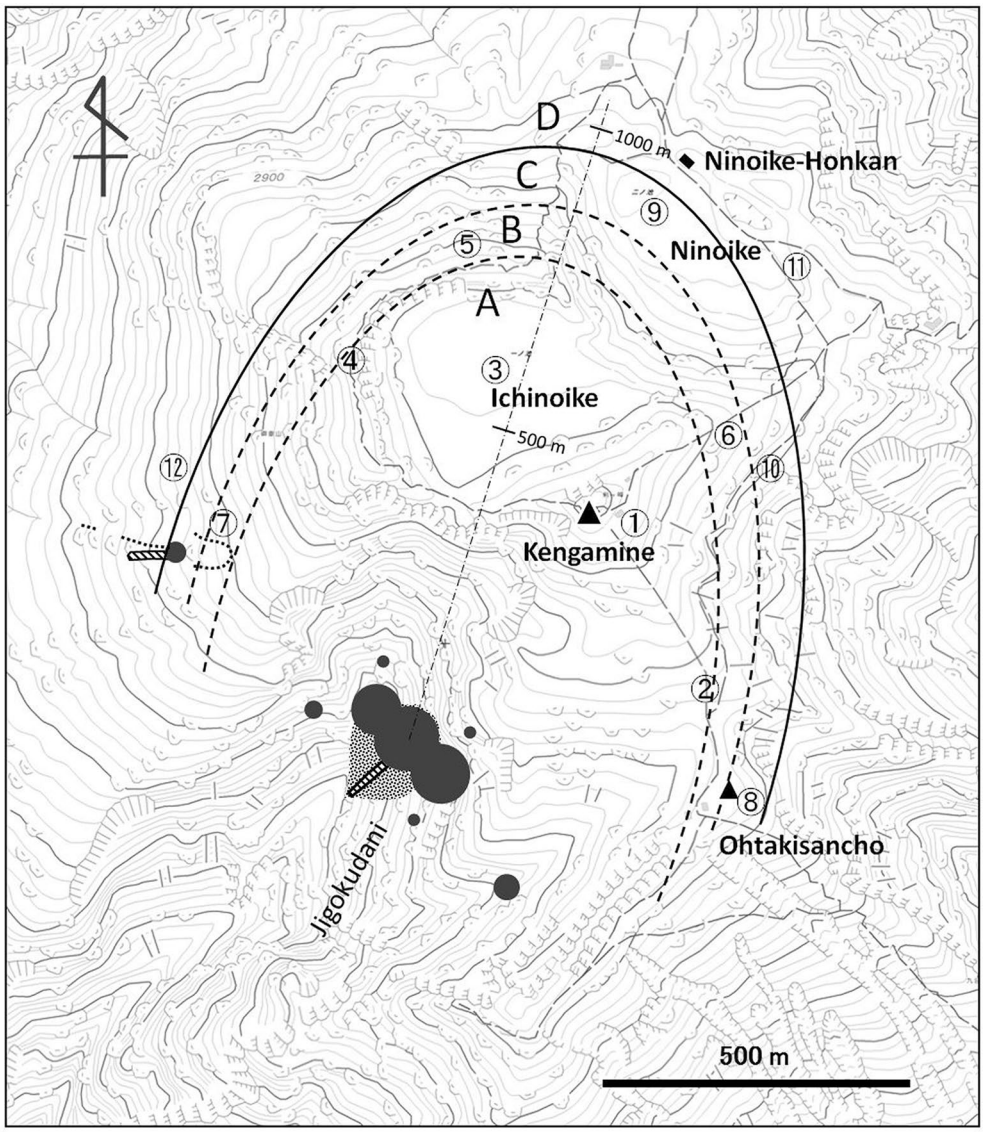

Fig. 6 Distribution of impact craters generated by ballistic ejecta. *Zone A*: $N \geq 10$ impact craters per 5 × 5 m, *Zone B*: $9 \geq N \geq 3$, *Zone C*: $2 \geq N > 0$, *Zone D*: $N = 0$. The *dotted line in the middle* shows the long axis of the distribution of impact craters. The topographic base map was produced using a GSI map issued by the Geospatial Information Authority of Japan

Relationship between the occurrence of the eruption plume and impacts of ballistic ejecta

The eruption plume increased in size shortly after the eruption and reached a height of several hundred meters above the summit (Kengamine; Fig. 9a). In that time, very little ballistic ejecta landed near the summit, where many people were killed on impact. Based on the time taken to reach a maximum height of approximately 11 km at 12:10 (Sato et al. 2015), the average upward speed of the eruption plume was estimated to be 400–500 m/min. If we assume that the altitude of the top of the eruption plume in the photograph shown in Fig. 9a was 3200 m, then this photograph is considered to have been taken about 1 min after the beginning of the eruption. Ballistic ejecta with the shortest flight durations are estimated to have landed on the summit (elevation: 3000 m; travel distance: 450 m) with a final velocity of 58 m/s about 7.7 s after ejection from the vent at an initial velocity of 93 m/s with an ejection angle 50° (Fig. 8b, case A). Ballistic ejecta with a maximum velocity of 111 m/s are estimated to have landed on the summit 18.5 s after ejection (ejection angle: 76°) with a final velocity of 79 m/s (Fig. 8b, case B), which is considered to represent the maximum flight duration. This means that large amounts of ballistic ejecta likely occurred several tens-of-seconds after the beginning of the eruption and that initially the

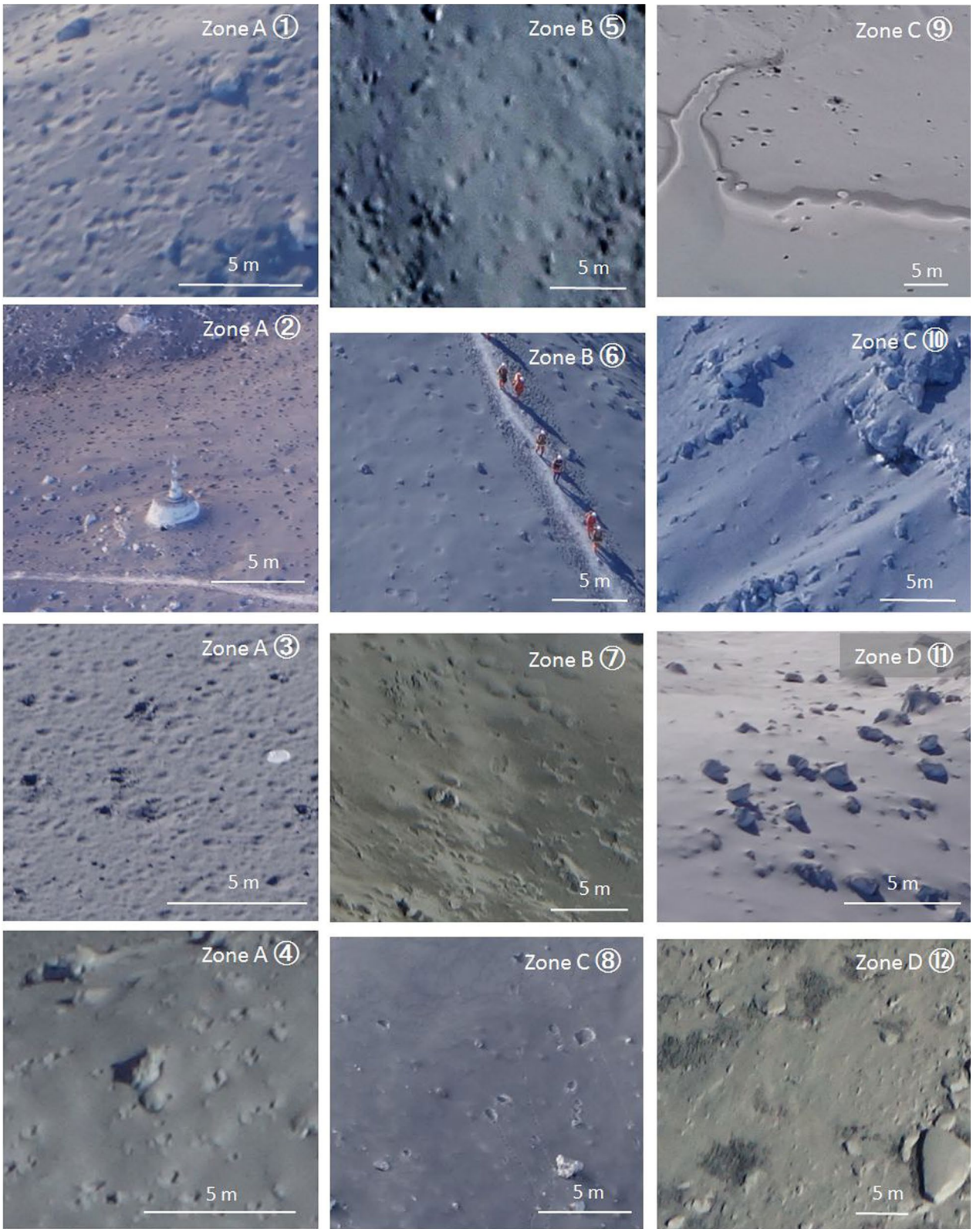

Fig. 7 Appearance of impact craters in each zone. *Numbers in circles* show the location of the areas in Fig. 6

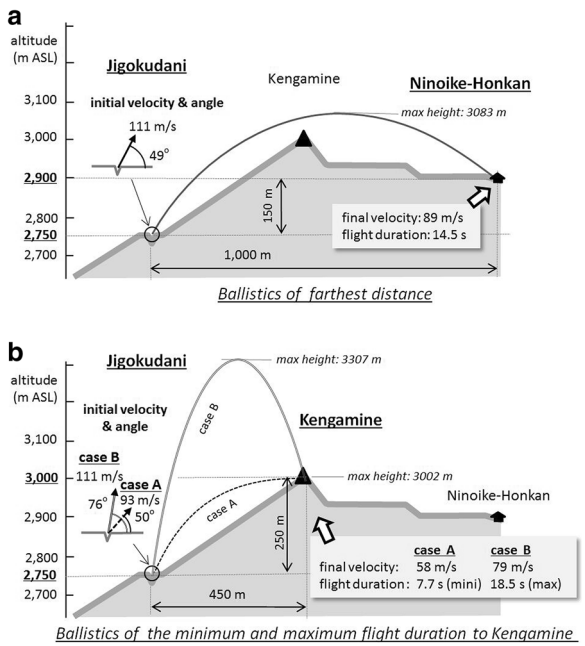

Fig. 8 Schematic illustrations showing the estimation of velocity and flight duration of ballistic ejecta based on the ballistic calculator software, "Eject!" (Mastin 2008). **a** Estimation of the initial velocity of ejecta that traveled the furthest. **b** Estimation of initial and final velocities and minimum and maximum flight durations of ballistic ejecta that traveled to Kengamine, where many people were killed on impact

eruption plume comprised a mixture of ash and gas that was ejected from the vents. This corroborates the eyewitness accounts of hikers at the summit who stated that the eruption plume rose soundlessly and that an explosion was only heard about 1 min after the beginning of the eruption (e.g., Tsuno 2014). The cluster of ballistic ejecta shown in Fig. 9b would have been the first cluster to land on the summit several seconds after this photograph was taken.

The volcanic tremor and inflation of the edifice that occurred 11 and 7 min before the eruption, respectively, are considered to have been caused by the sudden migration of the vapor phase, comprising water vapor and other gasses, to shallower depths (Kato et al. 2015). The initial phase of the eruption may therefore have been caused by the ejection of this vapor phase to the surface at 11:52 on September 27; however, the ejection of this gas phase did not generate large amounts of ballistic ejecta, probably because the intensity of the resulting explosion was too low. The removal of a large amount of the vapor phase from a hydrothermal reservoir in which the water–vapor system is in equilibrium can cause rapid boiling (bumping) of water due to a decrease in the boiling temperature via sudden decompression of the system (Taniguchi and Ueki 2014). This likely caused the explosive phase of the eruption, which then generated a cluster of ballistic ejecta, several tens-of-seconds after the initial phase of the eruption. The occurrence of rapid boiling and the accompanying explosions may have gradually propagated to the deeper parts of the hydrothermal system, resulting in the intermittent generation of ballistic ejecta during the explosive phase of the eruption, which continued for approximately 1 h.

Concluding remarks

We clarified the eruptive processes and mechanisms associated with the 2014 Mount Ontake eruption using aerial photographs taken the day after the eruption as

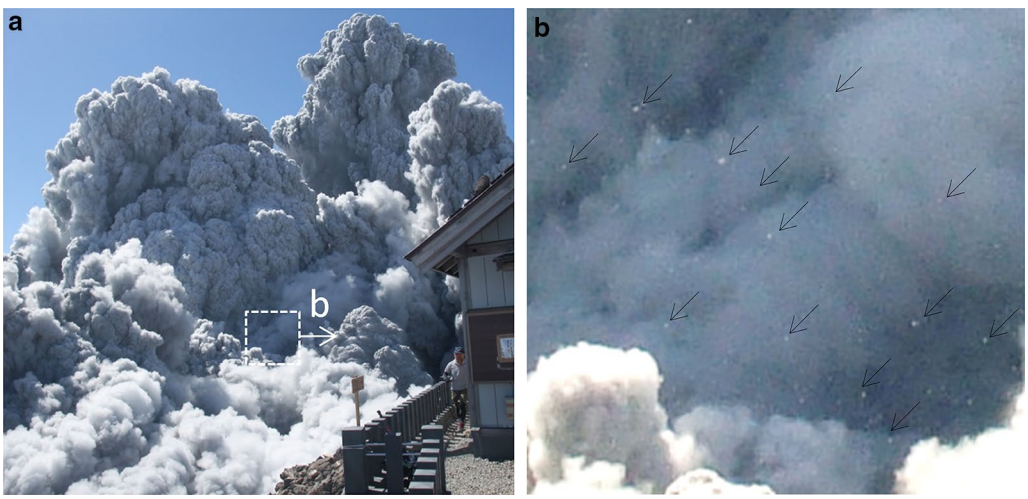

Fig. 9 **a** Growing eruption plume photographed immediately after the beginning of eruption. This photograph was taken by the late Noguchi I from Kengamine at the summit of Mt Ontake. **b** Close-up of the photograph. *Arrows* indicate a cluster of ballistics

well as other information. The conclusions of the study can be summarized as follows:

1. The vents involved in the eruption on the southwestern side of the summit are arranged along a west-northwest to east-southeast axis, which is subparallel to the axis of the vents involved in the 1979 eruption.
2. Among the three major vents on the floor of the Jigokudani valley, the vent at the center (J4) was the main vent involved in the eruption on September 27, with the other vents likely forming as a result of nonexplosive processes on the following day.
3. The pyroclastic flow travelled about 2.5 km along the Jigokudani valley at an average speed of 32 km/h. Since no burned or fallen trees were observed in this region, it appears that the temperature and destructive force associated with the pyroclastic flow were low.
4. The distribution of ballistic ejecta was inferred from impact craters, and the furthest impact crater was located 950 m from the vents, although the furthest ballistic was found at the mountain cottage, located 1000 m from the summit. Based on ballistic models, the maximum initial velocity of the ejecta was estimated to be 111 m/s.
5. Immediately after the beginning of the eruption, very few ballistic ejecta were observed around the summit, even though the eruption plume had risen above the summit. Based on this observation and the relationship between the speed of upward expansion of the eruption plume and the minimum flight duration of ballistic ejecta that landed on the summit, the generation of large amounts of ballistic ejecta is considered to have occurred several tens-of-seconds after the beginning of the eruption, probably in relation to the explosion mechanism of the hydrothermal reservoir deep under the volcano.

The results of this study show that, in the case of phreatic eruptions, there is a window of several tens-of-seconds before the first cluster of ballistic ejecta arrives. In the Mount Ontake 2014 eruption, ballistic analysis revealed that the final velocity of ejecta at the time of landing ranged between 58 and 79 m/s (209 and 284 km/h) near the summit. Anyone struck by such ejecta could be seriously injured. Thus, when hiking on volcanoes that have undergone repeated phreatic eruptions, it is important to minimize the amount of time spent near vents and to be aware of structures that can be used for protection, such as mountain cottages, large rocks, or shelters. Furthermore, in the event of an eruption, it is important to avoid centers of volcanic activity and to seek shelter during the time window before ballistic ejecta are generated.

Authors' contributions

TK took aerial photographs and analyzed them with FM. SN helped draft the manuscript. All authors read and approved the final manuscript.

Acknowledgements

We thank the Chunichi/Tokyo Shimbun Newspaper Co. and Usami A for the opportunity to observe the volcano from a helicopter and Noguchi H for permitting us to use photographs of the eruption that were taken by her husband, the late Noguchi I. We are also very grateful to the reviewers, Yoshimoto M, and an anonymous reviewer, whose comments were useful for improving the manuscript. This work was supported in part by a Grant-in-Aid for Scientific Research (A) from the Japan Society for the Promotion of Science KAKENHI (Grant No. 23241055 to TK).

Competing interests

The authors declare that they have no competing interests.

Received: 20 November 2015 Accepted: 20 April 2016
Published online: 03 May 2016

References

Asahi K (2014) Ontake eruption viewed at close range. Kagaku 84:1226–1227 **(in Japanese)**

Cabinet Office (2015) Handbook for improving the volcanic shelter. http://www.bousai.go.jp/kazan/shiryo/pdf/201512_hinan_tebiki4.pdf. Accepted Dec 2015 (**in Japanese**)

Cas RAF, Wright JV (1987) Volcanic successions: modern and ancient. Chapman & Hall, London

Japan Metrological Agency (2014) Ontakesan (September 2014 Issue). Monthly commentary documents on volcanic activity. http://www.data.jma.go.jp/svd/vois/data/tokyo/STOCK/monthly_v-act_doc/tokyo/14m09/312_14m09.pdf. Accepted Oct 2014 (**in Japanese**)

Kaito F (2014) Eyewitness testimony 3. In: Yamatokeikokusha (ed) Document of the Ontake eruption. Yama-Kei Publishers, Tokyo **(in Japanese)**

Kato K (2014) Eyewitness testimony 4. In: Yamatokeikokusha (ed) Document of the Ontake eruption. Yama-Kei Publishers, Tokyo **(in Japanese)**

Kato A, Terakawa T, Yamanaka Y, Maeda Y, Horikawa S, Matsuhiro K, Okuda T (2015) Preparatory and precursory processes leading up to the 2014 phreatic eruption of Mount Ontake, Japan. Earth Planets Space 67:111

Kobayashi T (1980) The 1979 activity of Ontake volcano, report for a grant from the Japanese Ministry of Education, Science and Culture (PI: H. Aoki), 4–12 (**in Japanese**)

Maeno F, Nakada S, Nagai M, Kozono T (2013) Ballistic ejecta and eruption condition of the vulcanian explosion of Shinmoedake volcano, Kyushu, Japan on 1 February, 2011. Earth Planets Space 65:609–621

Mastin LG (2008) A simple calculator of ballistic trajectories for blocks ejected during volcanic eruptions, version 1.4. US Geol Sur Open File Rep 01–45

Nakada S, Nagai M, Kaneko T, Nozawa A, Suzuki-Kamata K (2005) Chronology and products of the 2000 eruption of Miyakejima Volcano, Japan. Bulletin of Volcanology 67:205–218

Oikawa T (2008) Reinvestigation of the historical eruption and fumarolic activity records at Ontake Volcano, central Japan. Misunderstanding reports about the 774 AD and 1892 AD eruptions. Bull Geol Surv Jpn 59:203–210 **(in Japanese with English abstract)**

Oikawa T, Suzuki Y, Chiba T (2014) Eruption history and 2014 eruption of Ontake volcano. Kagaku 84:1218–1225 **(in Japanese)**

Oikawa T, Yamaoka K, Yoshimoto M, Nakada S, Takeshita Y, Maeno F, Ishizuka Y, Komiri J, Shimano T, Nakano S (2015) The 2014 eruption of Ontake volcano, central Japan. Bull Volcano Soc Jpn 60:411–415 **(in Japanese)**

Sato E et al (2015) Eruption of Ontake 2014 as observed from meteorological radar. Report of coordinating committee for prediction of volcanic eruptions, 119, http://www.data.jma.go.jp/svd/vois/data/tokyo/STOCK/kaisetsu/CCPVE/ccpve_bulletin.html. (in press) (**in Japanese**)

Taniguchi H, Ueki S (2014) What was going on under the Ontake volcano? Programme and abstracts, The Volcanological Society of Japan "Supplement: Emergency Academic Session". 2014 Fall Meeting, U19 (**in Japanese**)
Tsuno Y (2014) Eyewitness testimony 7. In: Yamatokeikokusha (ed) Document of the Ontake eruption. Yama-Kei Publishers, Tokyo **(in Japanese)**
Yamamoto T (2014) The pyroclastic density currents generated by the September 27, 2014 phreatic eruption of Ontake Volcano, Japan. Bull Geol Surv Japan 65:117–127 **(in Japanese with English abstract)**